

Supporting Information  
For

**Fine-tuning of the water oxidation performance of hierarchical  $\text{Co}_3\text{O}_4$   
nanostructures prepared from different cobalt precursors**

Pradnya M. Bodhankar,<sup>a,b</sup> Avani Chunduri,<sup>b</sup> Nainesh Patel,<sup>b</sup> Dattatray S. Dhawale,<sup>\*c</sup> Ajayan  
Vinu,<sup>d</sup> Hind Aljohani,<sup>e</sup> and Pradip B. Sarawade<sup>\*a,b</sup>

<sup>a</sup>National Centre for Nanoscience and Nanotechnology, University of Mumbai, Vidyanagari,  
Santacruz, Mumbai-400098, India

<sup>b</sup>Department of Physics, University of Mumbai, Vidyanagari, Santacruz, Mumbai-400098,  
India

<sup>c</sup>Global Innovative Centre for Advanced Nanomaterials, Faculty of Engineering and Built  
Environment, The University of Newcastle, University Drive, Callaghan NSW 2308 Australia

<sup>d</sup>Qatar Environment and Energy Research Institute (QEERI), Hamad Bin Khalifa University  
(HBKU), Qatar Foundation, P.O. Box 34110, Doha, Qatar

<sup>e</sup>King Abdullah University of Science and Technology, Jeddah, Western province, Saudi  
Arabia

Fax: (+91)2652 2222

pradip.sarawade@physics.mu.ac.in, dattatraydhawale@gmail.com

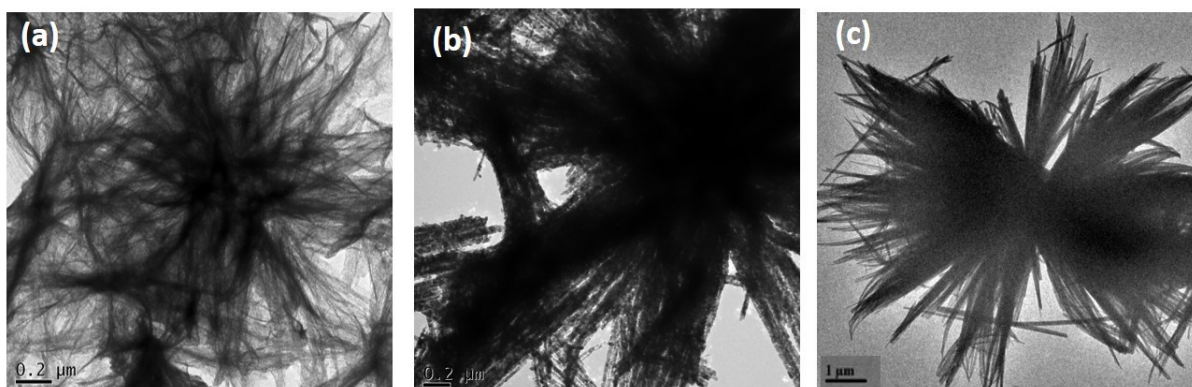


**Fig. S1.** Low and high magnification SEM and TEM images of  $\text{Co}_3\text{O}_4\text{-S}$  (a, b and c);  $\text{Co}_3\text{O}_4\text{-Ac}$  (d, e and f);  $\text{Co}_3\text{O}_4\text{-N}$  (g, h and i), respectively.

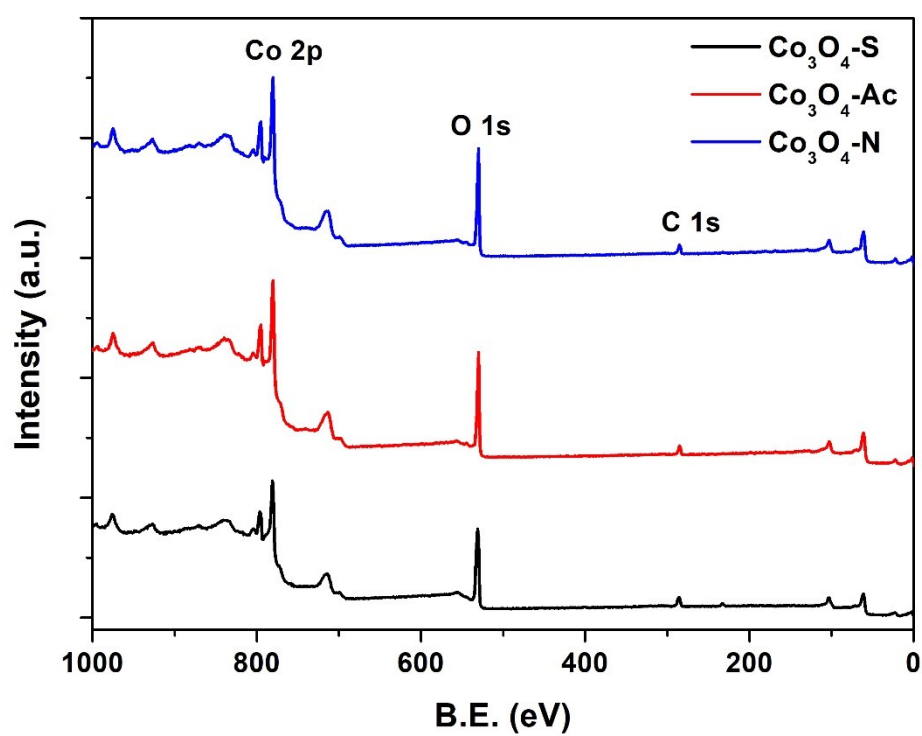


**Fig. S2.** XPS survey spectra of  $\text{Co}_3\text{O}_4\text{-S}$ ,  $\text{Co}_3\text{O}_4\text{-Ac}$  and  $\text{Co}_3\text{O}_4\text{-N}$  nanostructured catalyst.

**Table S1.** XPS surface atomic % of  $\text{Co}_3\text{O}_4\text{-S}$ ,  $\text{Co}_3\text{O}_4\text{-Ac}$  and  $\text{Co}_3\text{O}_4\text{-N}$  hierarchical nanostructured catalysts.

Catalyst	Surface atomic composition (%) from XPS		
	Co 2p	O 1s	C 1s
$\text{Co}_3\text{O}_4\text{-S}$	23.25	57.91	18.84
$\text{Co}_3\text{O}_4\text{-Ac}$	27.77	56.46	15.78
$\text{Co}_3\text{O}_4\text{-N}$	29.01	54.65	16.34

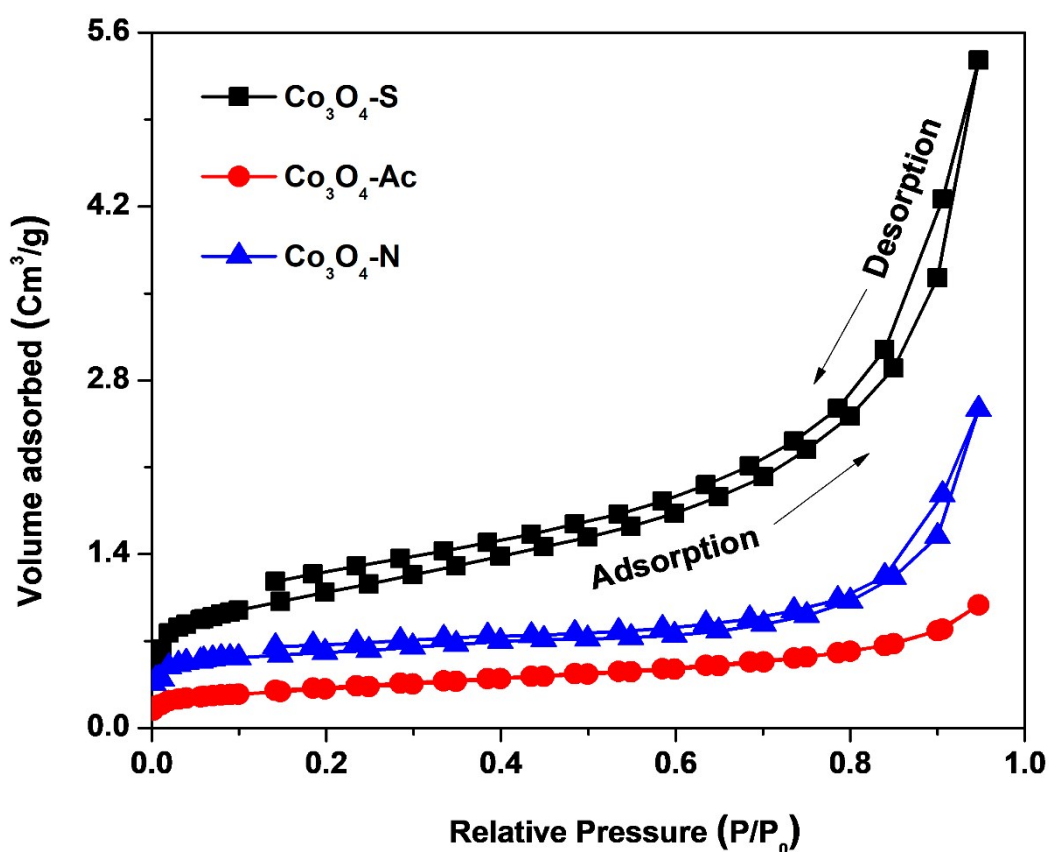


**Fig. S3.**  $\text{N}_2$  Adsorption-desorption isotherm of obtained from BET measurements for  $\text{Co}_3\text{O}_4\text{-S}$ ,  $\text{Co}_3\text{O}_4\text{-Ac}$  and  $\text{Co}_3\text{O}_4\text{-N}$  nanostructured catalyst.

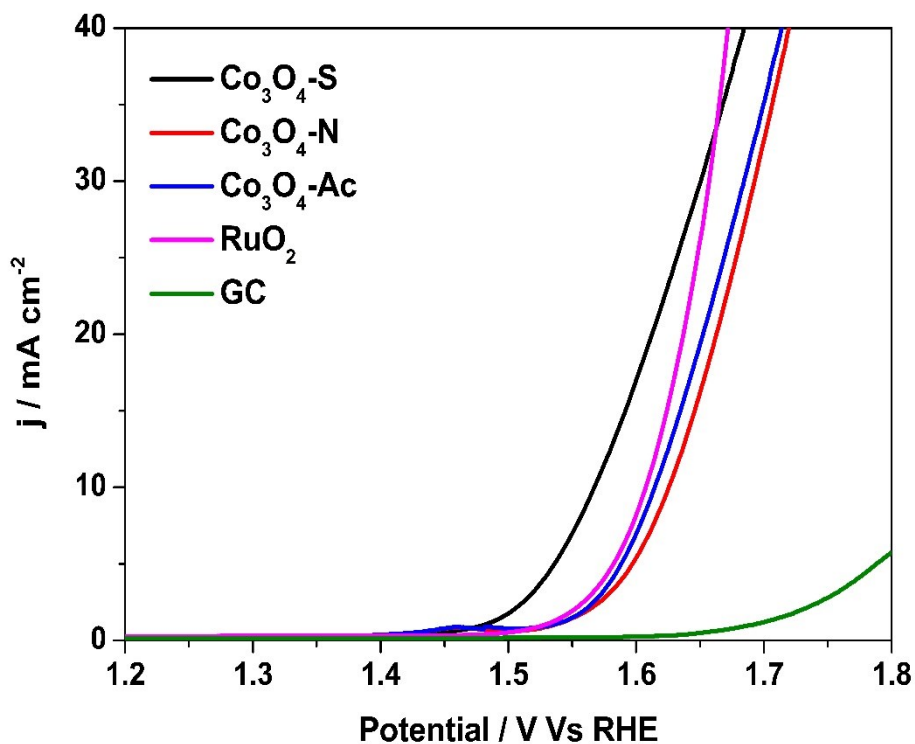


**Fig. S4.** Linear polarization curves (iR compensated) at a scan rate of 10 mV/s for  $\text{Co}_3\text{O}_4\text{-S}$ ,  $\text{Co}_3\text{O}_4\text{-Ac}$ ,  $\text{Co}_3\text{O}_4\text{-N}$ ,  $\text{RuO}_2$ , and GC.

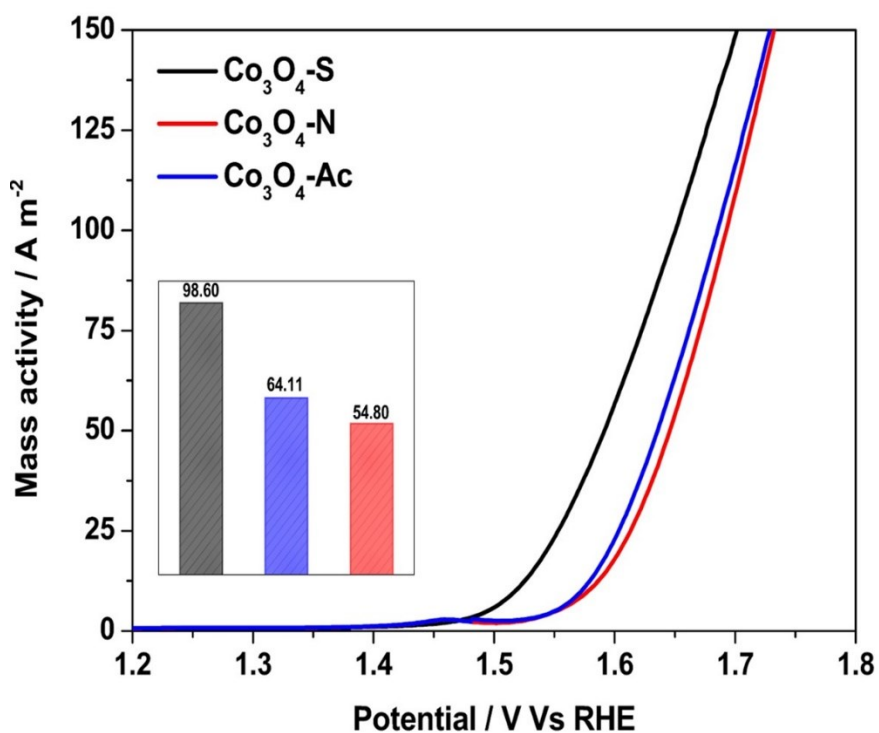


**Fig. S5.** Potential dependent mass activity curves for  $\text{Co}_3\text{O}_4\text{-S}$ ,  $\text{Co}_3\text{O}_4\text{-Ac}$ ,  $\text{Co}_3\text{O}_4\text{-N}$  (inset: a bar chart of the mass activity).

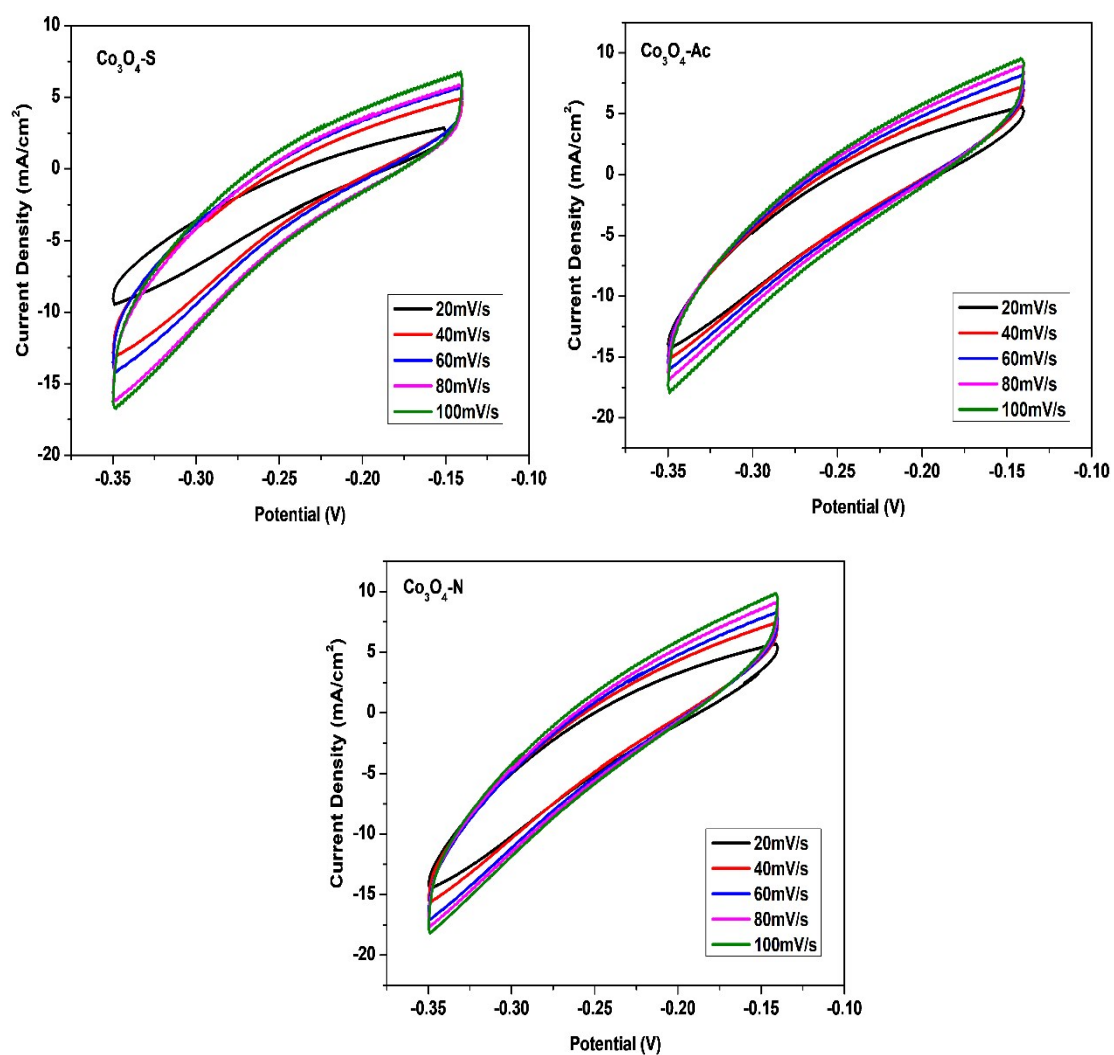


**Fig. S6.** CV curves at various scan rates to determine the double-layer capacitance (Cdl) of  $\text{Co}_3\text{O}_4\text{-S}$ ,  $\text{Co}_3\text{O}_4\text{-Ac}$  and  $\text{Co}_3\text{O}_4\text{-N}$  nanostructured catalysts.

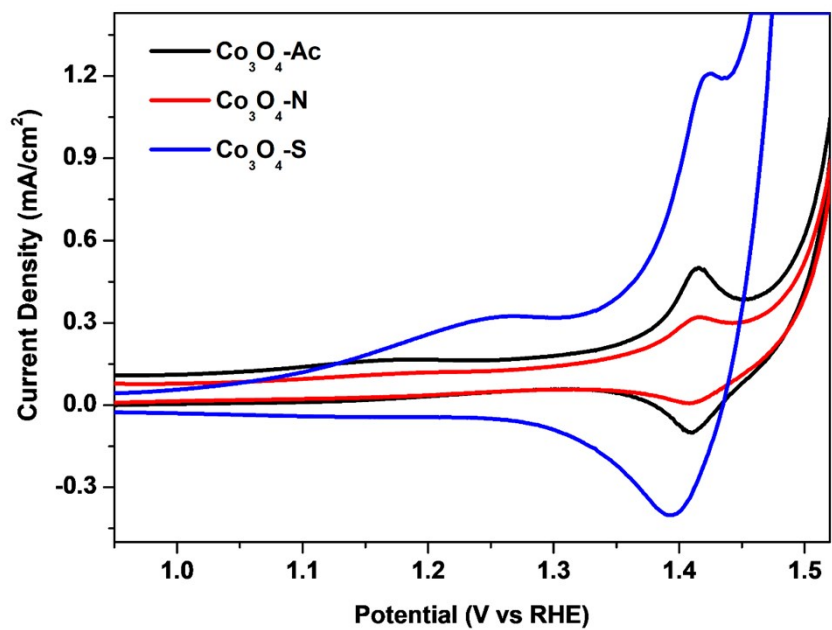


**Fig. S7.** Cyclic voltammetry scan for  $\text{Co}_3\text{O}_4\text{-S}$ ,  $\text{Co}_3\text{O}_4\text{-Ac}$  and  $\text{Co}_3\text{O}_4\text{-N}$  nanostructured catalysts at a scan rate of 2 mV/s in 1M KOH.

### **Electrochemically active surface area [(ECSA /cm<sup>2</sup>)]**

ECSA of each catalyst is measured from double layer charging of the catalytic material. Firstly, the non-faradaic region from CV scan is determined. Multiple CV curves at scan rate of 20, 40, 60, 80 and 100 mV/s are recorded. It is assumed that all the current in this region is due to double layer charging capacitance. Following this, a potential value in the middle region is identified and current associated with this potential value is plotted as a function of scan rate. The slope of which gives the value of double layer capacitance according to the equation given below;

$$i_c = v C_{dl}$$

where  $i_c$  is the double layer charging current,  $v$  is scan rate and  $C_{dl}$  is double layer charging capacitance. The electrochemically active surface area is calculated from the following relation;

$$ECSA = \frac{C_{dl}}{C_s}$$

Here,  $C_s$  is the specific capacitance of the sample or the capacitance of an atomically smooth planer surface of the material per unit area under identical electrolyte conditions. The value of the specific capacitance for various metal electrodes in alkaline electrolyte have been measured and typical reported value lies in the range from 0.022 to 0.130 mF cm<sup>-2</sup> in KOH solution. We have considered the reported value of 0.027 mF cm<sup>-2</sup> for Co in alkaline solution and ECSA is calculated accordingly.<sup>1, 2</sup>

### **Mass activity [MA (A g<sup>-1</sup>)]**

MA was calculated using the following equation given below;

$$MA = \frac{J}{\text{Active mass of catalyst}}$$

Here,  $J$  is the current density in mA cm<sup>-2</sup> at specific overpotential value of 1.6 V for comparing the electrocatalytic activities of all hierarchical nanostructured electrocatalysts.<sup>3</sup>

### Turnover frequency [TOF (S<sup>-1</sup>)]

Following equation is used to calculate the TOF of electrochemical reaction.<sup>4</sup>

$$TOF = \frac{j * N_A}{n * A * F * \Gamma}$$

Where,

j = Current density (A/m<sup>2</sup>) at a specified overpotential value.

N<sub>A</sub> = Avogadro's constant [6.022\*10<sup>23</sup>].

n = Number of electrons.

A= Electroactive surface area.

F = Faraday constant [96485 C].

Γ = Surface concentration of atom on the electrode surface.

### Surface concentration of Co<sub>3</sub>O<sub>4</sub>-S from CV curve

Charge passed calculated by integrating the area under reduction peak from potential vs. current curve.

Calculated area associated with the reduction of Co<sup>3+</sup> to Co<sup>2+</sup> = 0.0471\*10<sup>-3</sup> VA

Hence, associated charge = 0.0471\*10<sup>-3</sup> VA / 0.002 V/s

$$= 0.02355 \text{ As}$$

$$= 0.02355 \text{ C}$$

The number of electrons transferred = 0.02355 C / 1.602\*10<sup>-19</sup> C

$$= 0.0147*10^{19}$$

Since, the reduction of Co<sup>3+</sup> to Co<sup>2+</sup> is a single electron transfer reaction, the number electrons calculated above is exactly the same as the number of surface active sites.

Hence, the surface concentration of Co<sup>2+</sup> that participated in OER is = 0.0147\*10<sup>19</sup>

$$TOF \text{ at } 1.53 \text{ V} = \frac{6.12 * 10^{-3} * 6.022 * 10^{23}}{4 * 0.089 * 96485 * 0.0147 * 10^{19}} = 0.7 \text{ s}^{-1}$$



**Table S2.** Exchange current density, ECSA, mass activity and TOF values of  $\text{Co}_3\text{O}_4\text{-S}$ ,  $\text{Co}_3\text{O}_4\text{-Ac}$  and  $\text{Co}_3\text{O}_4\text{-N}$  hierarchical nanostructured catalysts.

Catalyst	Exchange current density ( $\text{A cm}^{-2}$ )	ECSA ( $\text{cm}^2$ )	Mass activity ( $\text{A g}^{-1}$ ) at 1.65 V Vs RHE	TOF ( $\text{s}^{-1}$ ) at 1.53 V Vs RHE
$\text{Co}_3\text{O}_4\text{-S}$	$1.723 \times 10^{-3}$	892	98.60	0.7
$\text{Co}_3\text{O}_4\text{-Ac}$	$1.682 \times 10^{-3}$	666	64.11	0.2
$\text{Co}_3\text{O}_4\text{-N}$	$1.698 \times 10^{-3}$	574	54.80	0.1

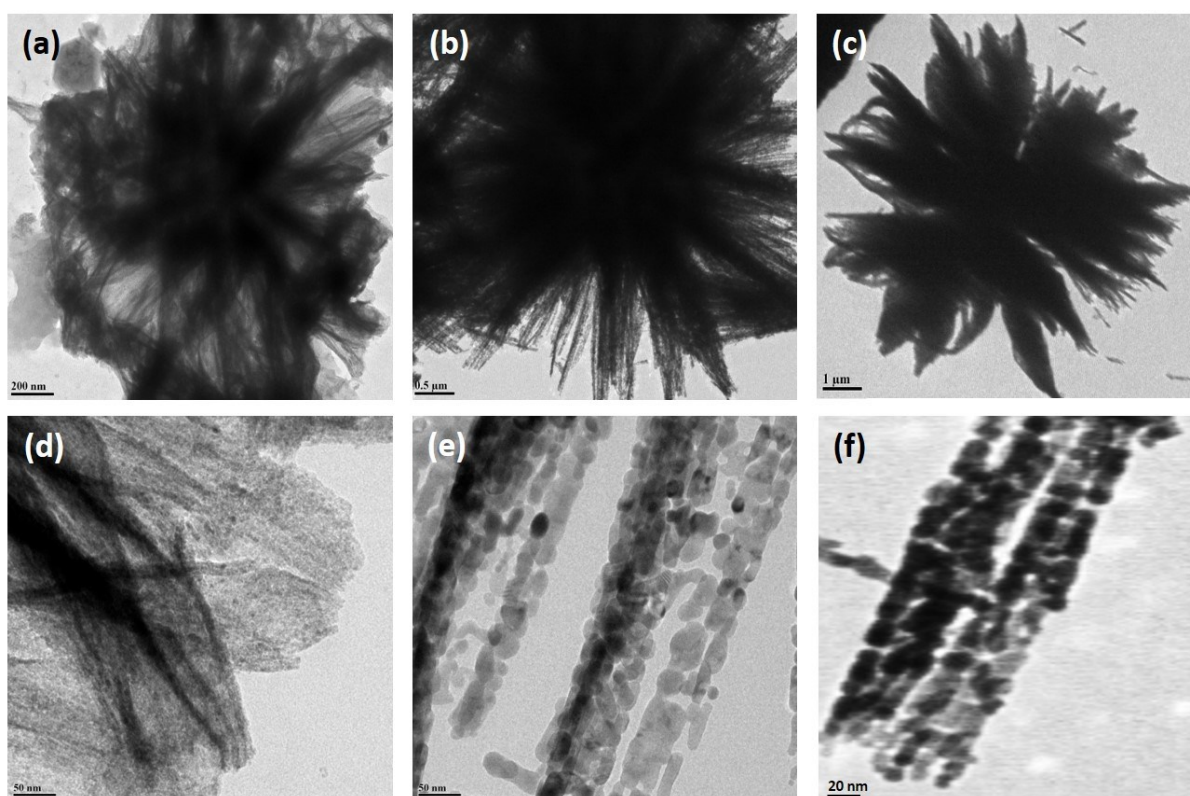


**Fig. S8.** Post-OER low and high magnification TEM image of  $\text{Co}_3\text{O}_4\text{-S}$  (a & d),  $\text{Co}_3\text{O}_4\text{-Ac}$  (b & e) and  $\text{Co}_3\text{O}_4\text{-N}$  (c & f) respectively.

**Table S3:** Comparison of recent Co based electrocatalysts for OER active in alkaline media.

Catalyst	Morphology	Electrolyte	Onset potential	Over-potential	Tafel slope	Ref.
----------	------------	-------------	-----------------	----------------	-------------	------

			(V)	(mV) at 10 mA cm <sup>-2</sup>		
AuCoCu alloy	Branched nanostructure	0.1M KOH	1.57	596	60	5
Ni <sub>0.7</sub> Co <sub>0.3</sub> O <sub>x</sub>	Hexagon nanoplate	0.1M KOH	1.62	394	-	6
Ce-MnCo <sub>2</sub> O <sub>4</sub>	Microrod	1M KOH	-	390	125	7
CuCoO <sub>2</sub>	Nanoplate	1M KOH	1.55	390	70	8
Co-Nitrogen co-doped Graphene	Nanosheet	0.1M KOH	-	426	69	9
Co <sub>1-x</sub> S/N-S-G	Crumpled, silk-like	0.1M KOH	-	371	63	10
Co <sub>3</sub> O <sub>4</sub> @BP	Lamellar	1M KOH	-	400	128	11
CeO <sub>2</sub> /Co <sub>3</sub> O <sub>4</sub>	Spherical	0.3M KOH	-	386	165.7	12
Co <sub>3</sub> V <sub>2</sub> O <sub>8</sub>	Nanoparticles	1M KOH	1.58	359	65	13
Co <sub>3</sub> O <sub>4</sub>	Semi spherical	1M KOH	1.52	425	44	14
Co <sub>3</sub> O <sub>4</sub>	flower-shaped	1M NaOH	1.51	356	68	15
Co <sub>3</sub> O <sub>4</sub>	Thin film	1M NaOH	-	377	58.1	16
Co <sub>3</sub> O <sub>4</sub> -F127	Sheetlike	1 M NaOH	-	350	90	17
Co <sub>3</sub> O <sub>4</sub>	Nanosheets	1M KOH	1.52	374	60	18
Porous Co <sub>3</sub> O <sub>4</sub>	Wrinkled shee-tlike	1M KOH	1.48	368	59	19
Co <sub>3</sub> O <sub>4</sub>	Nanoflakes	1M KOH	1.60	380	46	20
Co@NS/CN Ts-MCFs	Hybrid fibers	0.1M KOH	1.53	362	54	21
Co <sub>3</sub> O <sub>4</sub> @GF_	Flat sheets	1M KOH	0.82 V	440	60.3	22

KMnO <sub>4</sub>						
Co-N/Co-O@N-C nanohybrid	Hierarchical porous nanoarchitecture	0.1M KOH	-	370	81.12	23
LiCoO <sub>2</sub>	-	0.1M KOH	1.55	350	52	24
Co <sub>3</sub> O <sub>4</sub> -S	Marigold flower-like	1M KOH	1.45	330	78	This work
Co <sub>3</sub> O <sub>4</sub> -Ac	Self-assembled flower	1M KOH	1.54	380	86	This work
Co <sub>3</sub> O <sub>4</sub> -N	Urchin-like	1M KOH	1.55	390	90	This work

## References

1. G. Wu, N. Li, D.-R. Zhou, K. Mitsuo and B.-Q. Xu, *Journal of Solid State Chemistry*, 2004, **177**, 3682-3692.
2. C. C. McCrory, S. Jung, J. C. Peters and T. F. Jaramillo, *Journal of the American Chemical Society*, 2013, **135**, 16977-16987.
3. N.-U.-A. Babar and K. S. Joya, *ACS Omega*, 2020.
4. S. Anantharaj, S. Ede, K. Karthick, S. S. Sankar, K. Sangeetha, P. Karthik and S. Kundu, *Energy & Environmental Science*, 2018, **11**, 744-771.
5. H. Gong, W. Zhang, F. Li and R. Yang, *Electrochimica Acta*, 2017, **252**, 261-267.
6. J. Chi, H. Yu, G. Li, L. Fu, J. Jia, X. Gao, B. Yi and Z. Shao, *RSC advances*, 2016, **6**, 90397-90400.
7. X. Huang, H. Zheng, G. Lu, P. Wang, L. Xing, J. Wang and G. Wang, *ACS Sustainable Chemistry & Engineering*, 2018, **7**, 1169-1177.
8. D. Xiong, Z. Du, H. Li, J. Xu, J. Li, X. Zhao and L. Liu, *ACS Sustainable Chemistry & Engineering*, 2018, **7**, 1493-1501.
9. X. Qiao, S. Liao, R. Zheng, Y. Deng, H. Song and L. Du, *ACS Sustainable Chemistry & Engineering*, 2016, **4**, 4131-4136.
10. X. Qiao, J. Jin, H. Fan, Y. Li and S. Liao, *Journal of Materials Chemistry A*, 2017, **5**, 12354-12360.
11. F. Shi, K. Huang, Y. Wang, W. Zhang, L. Li, X. Wang and S. Feng, *ACS applied materials & interfaces*, 2019, **11**, 17459-17466.
12. S. A. Khan, S. B. Khan and A. M. Asiri, *Journal of Materials Science: Materials in Electronics*, 2016, **27**, 5294-5302.
13. M. Xing, L.-B. Kong, M.-C. Liu, L.-Y. Liu, L. Kang and Y.-C. Luo, *Journal of Materials Chemistry A*, 2014, **2**, 18435-18443.
14. S. Asadzadeh, M. Amirnasr, S. Meghdadi, F. F. Tirani and K. Schenk, *International Journal of Hydrogen Energy*, 2018, **43**, 4922-4931.

15. C. Ranaweera, C. Zhang, S. Bhojate, P. Kahol, M. Ghimire, S. Mishra, F. Perez, B. K. Gupta and R. K. Gupta, *Materials Chemistry Frontiers*, 2017, **1**, 1580-1584.
16. H. S. Jeon, M. S. Jee, H. Kim, S. J. Ahn, Y. J. Hwang and B. K. Min, *ACS applied materials & interfaces*, 2015, **7**, 24550-24555.
17. P. Jash, V. Aravind and A. Paul, *New Journal of Chemistry*, 2019, **43**, 6540-6548.
18. B. Sidhureddy, J. S. Dondapati and A. Chen, *Chemical communications*, 2019, **55**, 3626-3629.
19. Z. Li, X.-Y. Yu and U. Paik, *Journal of Power Sources*, 2016, **310**, 41-46.
20. S. Chen, Y. Zhao, B. Sun, Z. Ao, X. Xie, Y. Wei and G. Wang, *ACS applied materials & interfaces*, 2015, **7**, 3306-3313.
21. Z. Wang, S. Peng, Y. Hu, L. Li, T. Yan, G. Yang, D. Ji, M. Srinivasan, Z. Pan and S. Ramakrishna, *Journal of Materials Chemistry A*, 2017, **5**, 4949-4961.
22. M. P. Araújo, M. Nunes, I. M. Rocha, M. Pereira and C. Freire, *ChemistrySelect*, 2018, **3**, 10064-10076.
23. K. J. Lee, D. Y. Shin, A. Byeon, A. Lim, Y. S. Jo, A. Begley, D.-H. Lim, Y.-E. Sung, H. S. Park and K. H. Chae, *Nanoscale*, 2017, **9**, 15846-15855.
24. T. Maiyalagan, K. A. Jarvis, S. Therese, P. J. Ferreira and A. Manthiram, *Nature communications*, 2014, **5**, 1-8.